Published in final edited form as:

Neuron. 1994 October ; 13(4): 823–835.

The Drosophila Tumor Suppressor Gene *dlg* Is Required for Normal Synaptic Bouton Structure

Timothy Lahey, **Michael Gorczyca**, **Xi-Xi Jia**, and **Vivian Budnik**

Department of Biology, Neuroscience and Behavior Program, University of Massachusetts, Amherst, Massachusetts 01003

Summary

The Drosophila tumor suppressor gene lethal (1) *discs large* (*dlg*) encodes a protein necessary for normal cell growth in epithelial and brain tissue. It shares high sequence identity to the mammalian synaptic proteins PSD-95 and SAP-70, whose functions are unknown. To determine the localization and role of dlg at synapses, we investigated its distribution and the effects of *dlg* mutations on Drosophila neuromuscular junctions. We show that dlg immunoreactivity is expressed at one type of glutamatergic synapse and is associated with both presynaptic and postsynaptic membranes. Mutations in *dlg* alter the expression of dlg and cause striking changes in the structure of the subsynaptic reticulum, a postsynaptic specialization at these synapses. These results indicate that *dlg* is required for normal synaptic structure and offer insights regarding the role of *dlg* homologs at vertebrate synapses.

Introduction

Synapses are complex structures that serve as the site of communication between neurons and their targets. A crucial step in understanding how synapses develop and how they are modified has been to identify their structural and functional components. Over the last several years, an increasingly large number of molecules that localize to the synapse has been identified, using biochemical and molecular methods (e.g., Südhof and Jahn, 1991; Ushkaryov et al., 1992). These components include cytoskeletal elements, membrane receptors, ion channels, extracellular matrix molecules, and constituents of second messenger cascades (reviewed by Hall and Sanes, 1993, for vertebrate neuromuscular junctions). The role of many of these elements in synaptic physiology and development has remained obscure. One reason for this has been the lack of an in vivo system in which the expression of these molecules can be specifically altered during development.

The Drosophila larval neuromuscular junction has been an increasingly popular model system to study synapse development and function (reviewed by Keshishian and Chiba, 1993). Synaptic endings at these muscles are easily accessible and exhibit stereotypic distribution and morphology, allowing the use of a genetic approach to pursue questions regarding developmental and functional aspects of the synapse. For example, the recent isolation of mutants affecting the Drosophila *synaptotagmin* gene, which shares 57% identity with the vertebrate counterpart, has allowed a direct examination of the role of this molecule in synaptic transmission at larval neuromuscular synapses (DiAntonio et al., 1993; Littleton et al., 1993).

Recent studies at mammalian central synapses have indicated that a major protein component of the brain postsynaptic density, PSD-95, shares high homology with a product of the Drosophila tumor suppressor gene *lethal (1) discs large (dlg-A)* (Cho et al., 1992; Woods and Bryant, 1991, 1993a). The protein SAP-90 has a deduced amino acid sequence identical to PSD-95 and has been localized to cerebellar presynaptic sites (Kistner et al., 1993). PSD-95 (or SAP-90) and dlg-A share 58% overall identity. dlg-A also shares 26% identity with the human tight junction protein ZO-1 (Willott et al., 1993), and the dlg protein is expressed at fly epithelial septate junctions, which are believed to be similar to vertebrate tight junctions (Woods and Bryant, 1991, 1993b). Mutations in the *dlg* locus result in neoplastic growth of larval imaginal discs, defective adhesion between epithelial cells, and abnormal cell polarity (Stewart et al., 1972; Woods and Bryant, 1991).

dlg protein is also observed at the neuropil in the fly CNS, and mutations in the *dlg* locus result in brain tumors. However, the function of *dlg* in the nervous system, as well as its subcellular localization, are not known. Similarly, the function of PSD-95 and SAP-90 at mammalian synapses has not been determined.

The deduced amino acid sequence of the dlg-A protein defines three domains shared by all members of this family of proteins. These include a domain homologous to a yeast guanylate kinase (Berger et al., 1989), a domain with close homology to the SH3 motif characteristic of signal transduction and cytoskeletal proteins, as well as nonreceptor tyrosine kinases (Mayer et al., 1988), and a 90 amino acid internal repeat sequence (GLGF repeats) of unknown function at the N-terminal half of the protein (Cho et al., 1992; Willott et al., 1993). The N-terminus region of the Drosophila protein is also homologous to collagen α chain (Ramirez et al., 1990; Woods and Bryant, 1991). Mutations affecting each of these domains have been isolated (Perrimon, 1988; Woods and Bryant, 1991).

To investigate the neural function of *dlg*, we examined the expression of its product at Drosophila larval neuromuscular junctions. In addition, we studied the effects of mutations in each of the three conserved domains on synaptic structure. We found that dlg was localized to a class of glutamatergic synapses, type I, at the Drosophila larval neuromuscular junction and was associated with presynaptic and postsynaptic membranes. In addition, we demonstrated that mutations in each of the three domains result in dramatic changes in postsynaptic structure. These results indicate that the *dlg* locus is required for normal synapse structure and may provide insight into the function of the *dlg* homolog PSD-95/SAP-90 at mammalian synapses.

Results

dlg Is Expressed at a Subset of Drosophila Neuromuscular Synapses

A polyclonal antibody directed against the SH3 and guanylate kinase domains of recombinant dlg-A (Woods and Bryant, 1991) was used to stain Drosophila larval neuromuscular junctions. Strong dlg immunoreactivity was observed at a subset of synaptic boutons in all 30 body wall muscle fibers per abdominal hemisegment (Figure 1A). In wild type, all abdominal body wall muscle fibers are innervated by motor endings containing 3–8 μm synaptic boutons (type I boutons). These boutons have been reported to contain

glutamate, the main excitatory transmitter at the larval neuromuscular junction (Jan and Jan, 1976; Johansen et al., 1989). In addition to glutamatergic innervation, subsets of body wall muscles are also innervated by nerve endings containing other putative transmitters or neuromodulators (Anderson et al., 1988; Cantera and Nässel, 1992; Gorczyca et al., 1993). Each of these endings has a characteristic synaptic bouton morphology and distribution in the muscles distinct from type I endings (Figure 1B).

Two kinds of type I boutons that differ in size and synaptic ultrastructure have been described (Atwood et al., 1993; Jia et al., 1993). Type Ib boutons are larger than type Is and are filled with 40 nm clear vesicles thought to contain glutamate (Johansen et al., 1989). At the postsynaptic site, type Ib boutons are surrounded by an elaborate system of membranes, the subsynaptic reticulum (SSR; Budnik et al., 1990; Atwood et al., 1993; Jia et al., 1993). Type Is boutons contain dense vesicles in addition to small clear vesicles and are surrounded by a less developed SSR (Atwood et al., 1993; Jia et al., 1993). dlg immunoreactivity was strong at type Ib boutons in all muscle fibers and much dimmer at type Is (Figure 1A). The specificity of this immunoreactivity was confirmed by the *dlg* mutant analysis, since at least one of the *dlg* mutant alleles, dlg^{m52}, eliminated the immunoreactivity (see below).

dlg-like immunoreactivity was also observed within type III synaptic boutons (see Figure 3C and below). These boutons innervate a single muscle fiber, muscle 12 (muscle nomenclature according to Crossley, 1978), in abdominal segments 2–5. None of the *dlg* alleles affected the staining at these boutons, which we interpret as cross-reactivity with another antigen or a *dlg* gene product not affected by the mutant alleles used (see Figure 3B). Type II boutons, which innervate most body wall muscle fibers, were devoid of immunoreactivity, as confirmed by double labeling with an antinervous system antibody, anti-horseradish peroxidase (anti-HRP) (Jan and Jan, 1982), which stains all bouton types (Figure 1B; Budnik et al., 1990).

Confocal microscopy of dlg-containing boutons revealed that immunoreactivity was concentrated at the peripheral border of type I boutons and in a “perisynaptic network” surrounding most of the bouton (Figure 1C). No detectable immunoreactivity was observed in the core of the bouton. Our immunoelectron microscopical analysis, using dlg antibodies (see below), suggested that this perisynaptic network corresponds in part to the SSR at type I boutons.

dlg Is Concentrated at Type I Bouton Postsynaptic Specializations and in the Presynaptic Membrane

To examine the subcellular localization of dlg at type Ib boutons, we examined dlg immunoreactivity at the electron microscopical level. The ultrastructure of type Ib boutons has been extensively studied (Atwood et al., 1993; Jia et al., 1993). Unfortunately, high concentrations of glutaraldehyde in the fixation mixture completely eliminated dlg immunoreactivity. We therefore examined the ultrastructural distribution of dlg in paraformaldehyde fixed preparations containing low concentrations of glutaraldehyde (0.01%), thus sacrificing some structural detail. However, in these preparations, many synaptic bouton features such as synaptic densities, vesicles, mitochondria, and SSR could

be clearly distinguished. dlg immunoreactivity was visualized using the diaminobenzidine peroxidase reaction (Figure 2).

As described above, type Ib boutons contain small clear vesicles presumed to contain glutamate (Johansen et al., 1989; Atwood et al., 1993; Jia et al., 1993). Each bouton is invaginated into the muscle cell and may contain as many as 20 putative synaptic release sites (Atwood et al., 1993; Jia et al., 1993). At the post-synaptic muscle, type Ib boutons are surrounded by a complex system of highly convoluted membranes, the SSR. We found that most dlg immunoreactivity was associated with SSR membranes, as well as in pockets defined by the SSR membrane convolutions (Figure 2A). Immunoreactivity could also be observed associated with the presynaptic membrane, but no immunoreactivity appeared in the bouton core. These results suggest that the dlg-immunoreactive perisynaptic network observed in confocal microscopy at type Ib boutons (Figure 1C) corresponds to the SSR.

dlg Mutants Decrease or Eliminate Anti-dlg Immunoreactivity

To determine whether the antigen stained by dlg antibodies was the *dlg* gene product and to examine the effects of alterations in the dlg protein on synaptic structure, we studied three *dlg* mutant alleles that alter each of the three conserved *dlg-A* domains: dlg^{v59}, which eliminates most of the guanylate kinase domain; dlg^{m52}, a genetic null allele; and dlg^{m30}, which disrupts the SH3 domain (Woods and Bryant, 1991). These alleles die during early metamorphosis with neoplastic growth in imaginal discs and the CNS. Mutants were observed in heteroallelic combinations, or over a deficiency for the *dlg* locus, Df(1)N71 (Df). We found that the intensity of dlg immunoreactivity was consistently altered in dlg^{v59}/Df, $dlg^{m52}Df$, and dlg^{v59}/dlg^{m52}, but was unchanged in the control heterozygote *dlg*/+ (Figure 3). Alterations in label intensity were observed in dlg^{m30}/Df, but were less consistent than the other alleles.

In dlg^{m52}/Df, dlg immunoreactivity was almost completely eliminated, such that type Ib boutons could not be observed, or could be observed barely above background levels (Figure 3B). In dlg^{v59}/Df, the overall intensity of the signal was significantly decreased, but type Ib boutons were still stained. These results strongly suggest that the antigen stained with anti-dlg antibodies at type Ib boutons corresponds to a *dlg* gene product.

To substantiate further the identity of the protein stained by anti-dlg antibodies, Western blot analysis of wild-type and *dlg* mutant alleles was performed using body wall muscle extracts (Figure 3C). In wild type, three bands of about 108, 97, and 40 kDa appeared most intensely stained with dlg antibodies. The 108 and 97 kDa proteins were dramatically reduced in both dlg^{v59}/Df and dlg^{m52}/Df, but were less consistently affected in $dlg^{m30}Df$. In dlg^{v59}/Df, there was a 29-fold reduction in the 108 kDa protein and a 34-fold reduction in the 97 kDa protein. In dlg^{m52}/Df, the 108 kDa band was missing, and the 97 kDa band showed a 7-fold reduction. The 40 kDa band did not change in intensity in any of the mutant combinations. Interestingly, only two *dlg* transcripts, of 6.0 and 5.5 kb, have been found throughout the larval stages (Woods and Bryant, 1989), and the product of the largest transcript, *dlg-A*, has been reported to have a predicted molecular mass of about 102 kDa (Woods and Bryant, 1991). The changes observed in the expression of dlg in the different mutant alleles in body

wall muscle extracts, as well as the immunocytochemical data, are consistent with the idea that the protein(s) stained at the neuromuscular junction correspond to a *dlg* gene product(s).

Alterations in Synaptic Bouton Structure in *dlg* Mutants

For studies of dlg-expression, we used the alleles dlg^{v59}/Df and dlg^{m30}/Df, because in these alleles dlg immunoreactivity was well above background levels. The pattern of dlg immunoreactivity was studied in detail in 269 individual type Ib boutons in control samples and 130 type Ib boutons from mutant samples. For this, images from a single branch containing at least three to five boutons were acquired from muscle fiber 6 at abdominal segment 3 and 4 of each larva using confocal microscopy. The distribution of dlg immunoreactivity in the peripheral rim of the bouton and in the perisynaptic network was scored by examining thin confocal sections.

Clear alterations in the pattern of dlg immunoreactivity were found in both dlg^{v59}/Df and dlg^{m30}/Df. In control samples, dlg immunoreactivity was observed at the bouton border and in the perisynaptic network (Figure 4A; 95% of control boutons). In boutons from dlg^{v59}/Df preparations, immunoreactivity was still observed at the border of the boutons, but it was absent in the perisynaptic network (Figure 4B; perisynaptic network staining in only 4% of the boutons).

Several possibilities may explain these results. First, because overall dlg immunoreactivity is decreased in dlg^{v59}/Df, the absence of stained perisynaptic network may reflect the low levels of the protein in this structure. This possibility is somewhat unlikely because the immunoelectron microscopical analysis revealed that dlg immunoreactivity is heaviest at the SSR (see Figure 2), and immunoreactivity in dlg^{v59}/Df is well above background levels. In addition, similar alterations in the perisynaptic network are seen in dlg^{m30}/Df. Another possibility is that the perisynaptic network is absent or abnormal, or that the dlg protein has an abnormal distribution in these mutants. To address some of these possibilities, we used anti-HRP antibodies as an independent way to label type Ib boutons.

Anti-HRP antibodies stain the border of synaptic boutons and the perisynaptic network, as revealed by double-labeling experiments, using both anti-HRP and anti-dlg antibodies. However, the pattern of anti-HRP staining in the perisynaptic network is distinct from the anti-dlg pattern (Figures 4A and 4C). At this site, anti-HRP staining appears in a punctate pattern around type Ib boutons (Figures 4C and 4D).

The pattern of anti-HRP staining was also altered in dlg^{v59}/Df type Ib boutons. As in wild type, it stained the bouton core and border. Unlike wild type, however, it appeared as large clumps of immunoreactive material surrounding type Ib boutons (Figure 4D). The changes in anti-dlg and anti-HRP immunoreactivity suggest that in *dlg* mutants, there may be ultrastructural changes in the region surrounding the boutons, presumably in the SSR.

The SSR Is Altered in *dlg* Mutants

To determine whether the changes in HRP and dlg immunoreactivity in *dlg* mutants reflected changes in synaptic bouton ultrastructure, we examined serial thin sections of type Ib boutons by transmission electron microscopy. We were confident that major changes in

synaptic structure could be readily detected, because an extensive analysis of synaptic bouton ultrastructure, based on serial reconstructions, had been previously performed by us and others (Budnik et al., 1990; Atwood et al., 1993; Jia et al., 1993).

Systematic analysis of over 1,800 thin sections of three dlg^{v59}/Df samples and one $dlg^{m52}Df$ sample revealed that the SSR was abnormal in *dlg* mutants. These changes were readily apparent in every bouton examined (Figure 5; N = 23 serially sectioned boutons). In wild type, the SSR appears as a stack of convoluted membranes that surrounds the entire bouton and that is separated from the presynaptic bouton by a synaptic cleft (Figures 5A and 5C). These membranes form several layers around the bouton at the postsynaptic muscle. Each layer is highly convoluted, defining pockets and crests.

In dlg^{v59}/Df and dlg^{m52}/Df mutants, the SSR surrounded type Ib synaptic boutons as usual, but unlike wild type, mutant SSR was less extensive and less complex, showing reduced folding of the subsynaptic membranes (Figures 5B and 5D). Because of this reduction in the membrane convolutions, the mutant subsynaptic reticulum appeared in a highly concentric arrangement around the synaptic bouton. Figure 6 shows representative examples of the SSR in eight different wild-type and $dlg^{v59}Df$ boutons. These drawings were obtained by tracing the SSR from a transversal thin section at the midline of each bouton. In all wild-type boutons, the SSR was tortuously folded in a network that surrounded the entire bouton in most samples. In *dlg* mutants, the SSR was less convoluted and had a simpler appearance. These data are consistent with the confocal data showing anti-dlg immunoreactivity restricted to the bouton border and not far into the periphery.

To obtain a quantitative estimate of these changes, drawings were scanned, and the cross sectional SSR membrane length, as well as the degree of SSR convolution, was measured. The index of convolution was defined as the number of membrane segments in a sample area of 0.5 μm^2 that diverged from concentricity by more than 45° (see Experimental Procedures). In $dlg^{v59}Df$, there was a 52% reduction in the index of convolution (43.3 ± 3.4/μm^2 in wild type versus 20.7 ± 2.4/μm^2 in dlg^{v59}/Df[N = 10 boutons, 4 measures each]; $p < 0.001$). The total SSR cross sectional membrane length was also reduced in mutant larvae. In control boutons, the mean SSR length, normalized by the bouton cross sectional area, was 34.3 ± 5.4 μm^{-1}, while in dlg^{v59}/Df it was 20.5 ± 1.9 μm^{-1} (N = 10; $p < 0.001$). These measurements thus confirm our visual observations. No apparent changes were found at type II and III boutons in the mutants.

PSD-95-like Immunoreactivity Colocalizes with dlg Immunoreactivity at Type I Boutons

The rat postsynaptic density protein PSD-95 has been reported to have high homology with dlg-A (Cho et al., 1992). We therefore studied the expression of PSD-95 at larval neuromuscular junctions using polyclonal antibodies directed against bacterially expressed PSD-95 (Cho et al., 1992). We found that the staining pattern closely resembled dlg-like immunoreactivity (Figure 7). PSD-95-like immunoreactivity was strong in type Ib boutons and barely above background in type Is boutons at all body wall muscles. As with dlg immunoreactivity, anti-PSD-95 staining was found at the peripheral border of the synaptic bouton and in the muscle region surrounding the bouton (Figure 7B). Unlike anti-dlg staining, however, PSD-95-like immunoreactivity was more punctate and diffuse in the

region surrounding the bouton, with no clearly defined perisynaptic network (Figure 7B). No PSD 95-like immunoreactivity was found at type II and III boutons or epithelial cell borders. The PSD-95 protein appeared to be exclusively expressed at type I boutons and to a lesser extent at the CNS neuropil (data not shown).

As with dlg immunoreactivity, anti-PSD-95 staining was decreased or eliminated in *dlg* mutants. PSD-95 staining was undetectable in dlg^{m52}/Df neuromuscular junctions (Figure 7D) and barely above background in dlg^{v59}/Df. The high homology between dlg and PSD-95, their similar localization at the neuromuscular junction, and their decreased or absent immunoreactivity in a parallel fashion in two alleles of *dlg* suggest that anti-PSD-antibodies may also stain a *dlg* gene product.

Discussion

In this paper, we demonstrate that a product of the tumor suppressor gene *dlg* is present at identified synaptic boutons at the Drosophila neuromuscular junction. Confocal and electron microscopical studies show that dlg is associated with presynaptic and post-synaptic membranes at type I boutons, a glutamatergic-type synapse (Jan and Jan, 1976; Johansen et al., 1989). Mutations in three alleles of *dlg*, which alter different domains of the protein, cause striking alterations in the morphology of the postsynaptic specialization at type I boutons. The SSR appears substantially less extensive and less complex in the mutants.

Although the SSR is a prominent feature of the larval neuromuscular junction, its role is not known. One hypothesis is that the SSR is the equivalent of the junctional folds at the vertebrate neuromuscular junction, at which postsynaptic proteins such as receptors and postsynaptic channels are clustered and at which postsynaptic responses are terminated (reviewed by Hall and Sanes, 1993). Physiological studies demonstrate that glutamate receptors are clustered around type I boutons (Jan and Jan, 1976; Broadie and Bate, 1993). Furthermore, we have recently shown that another receptor, a Drosophila insulin receptor homolog, is clustered around type I boutons at the larval neuromuscular junction (Gorczyca et al., 1993). It is possible that the efficacy of the synaptic response could be regulated by changes in the morphology of the SSR. For example, a less convoluted membrane may provide less membrane surface for integration of receptors or for coupling the electrical signal to muscle contraction. Physiological studies will be required to determine the physiological consequences of the altered postsynaptic specialization in *dlg* mutants.

The studies in *dlg* mutants implicate the dlg protein in regulating the structure of the SSR. This role is consistent with several aspects of this protein (see below). dlg belongs to a family of intracellular proteins with several domains of homology to proteins associated with cell junctions (Woods and Bryant, 1991; Cho et al., 1992; Kistner et al., 1993; Willott et al., 1993; Woods and Bryant, 1993a). The predicted amino acid sequences that dlg shares with these related molecules include one to several 90 amino acid internal repeat sequences (GLGF repeats) of unknown function at the N-terminal half of the protein, an SH3 sequence, and a domain homologous to the yeast guanylate kinase at the carboxyl end. In addition, the dlg protein uniquely contains a PEST sequence and a region of homology to collagen α chain (Woods and Bryant, 1991).

SH3 domains, or Src-homology 3 domains, are sequences of about 45 amino acids, which are often found in proteins that comprise or associate with the cytoskeleton and the plasma membrane (reviewed by Koch et al., 1991; Pawson and Gish, 1992). It has been proposed that SH2 and SH3 domains function as adapter domains that transduce signals from tyrosine kinase growth factor receptors to other enzymes in a particular cytoplasmic pathway (Pawson and Gish, 1992; Smith et al., 1993). The fact that many SH3-containing proteins are cytoskeletal or cytoskeleton-associated proteins has led to the suggestion that they are involved in the organization and regulation of the cytoskeleton (Pawson and Gish, 1992). It is possible that dlg-A, as well as other SHS-containing proteins, interacts with the synaptic cytoskeleton, regulating its organization. This hypothesis is supported by our observation that mutations in the *dlg* locus produce dramatic changes in a postsynaptic structure at the neuromuscular junction.

Another domain common to all dlg-like proteins is an amino acid sequence with high homology to the yeast guanylate kinase, which catalyzes the conversion of GMP and ATP into GDP and ADP (Berger et al., 1989; Woods and Bryant, 1991). It has been suggested that one of the functions of this protein is to control the cellular ratio of GDP to GTP, thereby regulating the activation of G proteins (Cho et al., 1992). Small Ras-like G proteins are involved in the formation of membrane ruffles, actin stress fibers, focal adhesion, and mobilization of synaptic vesicles (Südhof and Jahn, 1991; Ridley and Hall, 1992; Ridley et al., 1992).

The dlg filamentous domain exhibits homology to collagen α chain. In Drosophila, the *dlg* gene product is also localized at the apical belt of lateral epithelial cell membranes, a cellular region coincident with septate junctions, thought to be the invertebrate analog of vertebrate tight junctions. Woods and Bryant (1991) have suggested that the filamentous domain could serve a structural function, perhaps forming the structure of septate junctions or interacting with membrane bound cytoskeleton. The filamentous domain could potentially contribute to structural aspects of synaptic boutons in the same way.

dlg-A and PSD-95 (or SAP-90) share 58% sequence identity (76% similarity; Cho et al., 1992; Kistner et al., 1993). This high degree of conservation, similar to that found in the synaptotagmin and myosin proteins in mammals and fruit flies (Perin et al., 1991; Bernstein et al., 1983), is a likely indication that the two proteins may have similar functions. In mammals, changes in postsynaptic structure have been implicated in the processes that follow long-term synaptic plasticity (Genisman et al., 1993). It would be interesting to know whether such changes are correlated with changes in PSD-95.

The similarity between dlg and PSD-95 was confirmed by our immunocytochemical studies, using antibodies against PSD-95. These studies demonstrated that type I boutons were also labeled by antibodies against PSD-95, that no PSD-95 immunoreactivity was observed at other bouton types, and that mutations in *dlg* decreased or eliminated the staining. However, unlike anti-dlg antibodies, no epithelial cell junctions were labeled by anti-PSD-95 antibodies. This result indicates that the anti-PSD-95 polyclonal antibody may recognize only a subset of the epitopes recognized by the anti-dlg polyclonal antibody. This

observation is consistent with the fact that the *dlg* locus encodes several transcripts (Woods and Bryant, 1991).

In general, anti-PSD-95 immunoreactivity was reduced to a greater degree than anti-dlg immunoreactivity. The difference in immunoreactivty using these two antibodies may simply reflect a difference in detection sensitivity, different background levels, or different epitopes on the antigen detected with these polyclonal antibodies.

An important issue is whether the dlg protein expressed at the neuromuscular junction is encoded by the *dlg* gene. In the present study, we found that anti-dlg immunoreactivity was most intense in three bands in Western blots of body wall muscle extracts. Two of these proteins (108 and 97 kDa) showed dramatic reductions in staining in two *dlg* alleles. A third band of 40 kDa did not appear to change in intensity or mobility in any of the *dlg* alleles examined. These results indicate that the 108 and 97 kDa proteins are likely to be *dlg* gene products. These proteins may represent two different products of the *dlg* gene generated by mRNA alternative splicing or posttranslational modification, or proteolytic cleavage of the protein during extract preparation. Woods and Bryant (1989) have already identified two *dlg* transcripts of 6.0 and 5.5 kb during the larval stages. These transcripts are already present in the first instar and are fairly abundant by the third instar (Woods and Bryant, 1989). A full or near full length *dlg* cDNA, which corresponds to the largest *dlg* transcript, has been sequenced. Its predicted molecular mass was reported to be about 102 kDa, in agreement with the results of this study. In the study of Woods and Bryant (1989), it was found that in the *dlg* allele dlg^{m52}, there was a new transcript of 4.0 kb. Interestingly, we found that a new lightly immunoreactive band at 92 kDa was observed in this allele.

The results of the Western blot analysis are also consistent with the immunocytochemical data, which show that dlg immunoreactivity is absent or dramatitally decreased in both dlg^{m52}/Df and dlg^{v59}/Df. No consistent alterations in the intensity of the bands was observed in dlg^{m30}/Df. However, a reduction in the immunoreactivity at neuromuscular junctions of dlg^{m30}/Df was seen, although less dramatic than in the other alleles. This discrepancy may be due to the fact that the dlg protein is subjected to different treatments for immunocytochemistry versus electrophoretie preparation, and that therefore, the epitopes may be somewhat altered. An additional band of 40 kDa that did not change in intensity was observed in all of the alleles. This protein may represent a cross-reacting antigen, such as the antigen stained at type III boutons, or a dlg gene product that is not altered by the mutant alleles used in this study.

The immunocytochemical studies of Woods and Bryant (1991) have demonstrated that dlg is expressed in epithelial cell borders and in the CNS neuropil. In this study, we have shown that dlg is also expressed at a subset of synapses at the neuromuscular junction. Whether these tissues express the same or different *dlg* transcripts will require examination by in situ hybridization using transcript-specific probes. However, so far only one of the *dlg* transcripts has been cloned and sequenced (Woods and Bryant, 1991).

In conclusion, we have shown that a product of the *dlg* locus is expressed at the neuromuscular junction, being concentrated at the postsynaptic specialization and at the

presynaptic membrane of a glutamatergic synapse. Mutations that alter three domains of dlg-A produce marked changes in the postsynaptic specialization, which are visible both at the light and electron microscopical level. These studies indicate that the *dlg* locus is important for normal synaptic structure.

Experimental Procedures

Fly Stocks

The *dlg* stocks dlg^{m52}, dlg^{v59}, and dlg^{m30} (provided by D. Woods and P. Bryant) were used for this study. These alleles were studied in heteroallelic combinations or over a deficiency for the region, Df(1)N71 (Df), obtained from the Bloomington Stock Center. The wild-type strain Canton Special (CS), or heterozygote animals *dlg/FM7* were used as control. We used *dlg* alleles over deficiency or in heteroallelic combinations to minimize the possible influence of second site recessive mutations on the phenotypes studied. The *dlg/Df* females used for these studies were obtained by crossing Df(1)N7l/Y; Dp (1:2) v[65b]/+ × *dlg/FM7*. Females that were *dlg/Df* were selected by the presence of large tumors in the brain and imaginal discs.

Immunocytochemistry

Larval body wall muscles were processed for immunocytochemistry as in Gorczyca et al. (1993), using 4% paraformaldehyde fixation and 0.2% Triton X-100 to permeabilize tissues. The following antibodies were used for this study: anti-HRP to label all synaptic bouton types at the larval neuromuscular junction (1:200 dilution; Gorczyca et al., 1993; Jan and Jan, 1982), anti-dlg (1:250; gift of D. Woods and P. Bryant), anti-PSD-95 (1:10; gift of M. Kennedy; Cho et al., 1992). As secondary antibodies, the following fluorescein isothiocyanate(FITC)-or Rhodamine-conjugated immunoglobulins were used: goat or donkey anti-rabbit IgG (Cappel and Chemicon, respectively) and donkey anti-goat IgG (Chemicon). Samples were observed under epifluorescence or confocal microscopy. Confocal images were acquired on a Bio-Rad MRC 600 attached to a Nikon microscope, processed with the NIH program image 1.5, and photographed from a computer screen.

The analysis of synapses using anti-dlg antibodies was based on 116 control and 81 *dlg* mutant samples. The analysis of synapses using PSD-95 antibodies was based on 12 control and 17 *dlg* mutants. The analysis of individual synaptic boutons by confocal microscopy was based on 269 control boutons and 130 dlg^{v59}/Df boutons. For the confocal analysis of individual boutons, type I boutons at muscle 6 in segments 3 or 4 were systematically acquired in each sample.

Western Blot Analysis

Protein extracts were prepared from larval body wall muscle prepartions, in which body wall muscles are attached to larval cuticle. Other tissues such as CNS, imaginal discs, salivary glands, pharyngeal apparatus, and gut were removed. About 10–20 body wall muscle preparations were collected in 50 μl of isolation buffer (2 μg/ml aprotinin, 2 μg/ml leupeptine, 2 μg/ml pepstatin, 100 μg/ml phenylmethylsulfonyl fluoride, 1% SDS, 0.5 mM EGTA, 150 mM NaCl, 10 mM phosphate buffer [pH 7.2]). Tissue was homogenized at 4°C

and cleared by centrifugation (1,900 × g for 10 min). Protein content was determined by the Bio-Rad microassay, using bovine serum albulmin (BSA) as a standard. An equal volume of 2× SDS sample buffer (Laemmli, 1970) was added to the muscle extract and boiled for 5 min. Samples containing 2 μg of protein were electrophoresed in 10% SDS–polyacrylamide gels. After electrophoretic separation, proteins were blotted onto a nylon membrane (Immobilon-P, Millipore) by electrotransfer. Blots were washed three times (10 min each) in PBST(150 mM NaCl, 0.05% Tween 20, 10 mM phosphate buffer [pH 7.2]), and blocked using 10% horse serum, 1% goat serum, 3% BSA, 2 mM sodium azide in PBST for 2 hr at room temperature. Blots were then incubated overnight in 1:1000 antidlg antibodies at room temperature, washed four times in PBST, and incubated in 1:1500 HRP-conjugated anti-rabbit antibody. Antibody complexes were visualized with an ELC chemoluminescence kit according to the directions of the manufacturer (Amersham). Gels were scanned using a UMAX UC630 scanner, and densitometric analysis was performed using the program Image 1.5.

Electron Microscopy

Samples were processed for transmission electron microscopy as in Jia et al. (1993). Synaptic boutons at muscles 6, 7, 12, and 13 in the third segment were serially sectioned and systematically photographed at 15,000× magnification. Three wild-type samples (1,200 serial sections; 18 type Ib boutons) and four *dlg* samples (three dlg^{v59}/Df and one dlg^{m52}/Df sample; 1,800 serial sections; 26 type I boutons) were used.

For immunoelectron microscopy, samples were fixed in 4% paraformaldehyde and 0.01% glutaraldehyde in 0.1 M phosphate buffer (pH 7.2) and processed for immunocytochemistry as above except that 0.1% Triton was used only during primary antibody incubation. The secondary antibody was HRP-conjugated anti-rabbit IgG (1:20 dilution). Two control samples were used for immunoelectron microscopical studies. As control, samples in which the primary antibody was omitted were processed in parallel with the anti-dlg-stained samples. No signal associated with synaptic boutons was observed in the control.

For the quantitative estimate of membrane length and SSR convolution, type Ib bouton SSR was traced from EM micrographs at 20,000× and then scanned for morphometrical analysis using a UMAX UC630 scanner. Pixels occupied by SSR membrane were counted using the NIH program Image 1.5 and converted to micrometers to calculate the cross-sectional SSR membrane length. The degree of SSR convolution in each scanned cross section was measured by selecting an area of 0.5 μm^2 of SSR adjacent to the presynaptic membrane. The angle of each membrane segment (>0.05 μm in length) with respect to the presynaptic membrane was calculated, using NIH Image 1.5. The number of SSR membrane segments that were more than 45° but less than 135° to the presynaptic membrane were counted (index of convolution). Four measurements of 0.5 μm^2 of SSR were taken at 90° axes for each bouton. Ten wild-type and ten dlg^{v59}/Df boutons were compared. Measurements were expressed as mean ± SEM and compared using Student's t-test.

Acknowledgments

We would like to thank Drs. E. Connor, R. Phillis, L. Schwartz, and D. Woods for helpful discussions. We also thank Drs. D. Woods, P. Bryant, and M. Kennedy for their generous gift of antibodies, and Dr. R. K. Murphey for lending us a diamond knife. This work was supported by NIH grant NS30072 and by an Alfred P. Sloan Fellowship to V. B.

References

Anderson MS, Halpern ME, Keshishian H. Identification of the neuropeptide transmitter proctolin in *Drosophila* larvae: characterization of fiber-specific neuromuscular endings. J. Neurosci. 1988; 8:242–255. [PubMed: 2892897]

Atwood H, Govind CK, Wu C-F. Differential ultra-structure of synaptic terminals on ventral longitudinal abdominal muscles in *Drosophila* larvae. J. Neurobiol. 1993; 24:1008–1024. [PubMed: 8409966]

Berger A, Schiltz E, Schulz GE. Guanylate kinase from *Saccharomyces cerevisiae*: isolation and characterization, crystallization and preliminary X-ray acid sequence and comparison with adenylate kinases. Eur. J. Biochem. 1989; 184:433–443. [PubMed: 2551688]

Bernstein SI, Mogami K, Donady JJ, Emerson CP Jr. *Drosophila* muscle myosin heavy chain encoded by a single gene in a cluster of muscle mutations. Nature. 1983; 302:393–397. [PubMed: 6403869]

Broadie K, Bate M. Synaptogenesis in the *Drosophila* embryo: innervation directs receptor synthesis and localization. Nature. 1993; 361:350–353. [PubMed: 8426654]

Budnik V, Zhong Y, Wu C-F. Morphological plasticity of motor axon terminals in *Drosophila* mutant with altered excitability. J. Neurosci. 1990; 10:3754–3768. [PubMed: 1700086]

Cantera R, Nässel DR. Segmental peptidergic innervation of abdominal targets in larval and adult dipteran insects revealed with an antiserum against leucokinin I. Cell Tissue Res. 1992; 269:459–471. [PubMed: 1423512]

Cho K-O, Hunt CA, Kennedy MB. The rat brain postsynaptic density fraction contains a homolog of the Drosophila disc-large tumor suppressor protein. Neuron. 1992; 9:929–942. [PubMed: 1419001]

Crossley, CA. The morphology and development of the *Drosophila* muscular system. In: Ashburner, M.; Wright, TRF., editors. The Genetics and Biology of *Drosophila*. Vol. 2b. New York: Academic Press; 1978. p. 499-560.

DiAntonio A, Parfitt KD, Schwartz TL. Synaptic transmission persists in *synaptotagmin* mutants of Drosophila. Cell. 1993; 73:1281–1290. [PubMed: 8100740]

Genisman Y, deToledo-Morrell F, Heller RE, Rossi M, Parshall RF. Structural synaptic correlate of long-term potentiation: formation of axiospinous synapses with multiple, completely partitioned transmission zones. Hippocampus. 1993; 3:435–446. [PubMed: 8269035]

Gorczyca MG, Augart C, Budnik V. Insulin-like receptor and insulin-like peptide are localized at neuromuscular junctions in *Drosophila*. J. Neurosci. 1993; 13:3692–3704. [PubMed: 8366341]

Hall ZW, Sanes JR. Synaptic structure and development: the neuromuscular junction. Cell 72/Neuron. 1993; 10:99–121.

Jan LY, Jan YN. l-glutamate as an excitatory transmitter at the *Drosophila* larval neuromuscular junction. J. Physiol. 1976; 262:215–236. [PubMed: 186587]

Jan LY, Jan YN. Antibodies to horseradish peroxidase as specific neuronal markers in *Drosophila* and grasshopper embryos. Proc. Natl. Acad. Sci. USA. 1982; 72:2700–2704. [PubMed: 6806816]

Jia X, Gorczyca M, Budnik V. Ultrastructure of neuromuscular junctions in *Drosophila*: comparison of wild type and mutants with increased excitability. J. Neurobiol. 1993; 24:1025–1044. [PubMed: 8409967]

Johansen J, Halpern ME, Johansen KM, Keshishian H. Stereotypic morphology of glutamatergic synapses on identified muscle cells of *Drosophila* larvae. J. Neurosci. 1989; 9:710–725. [PubMed: 2563766]

Keshishian H, Chiba A. Neuromuscular development in *Drosophila*: insights from single neurons and single genes. Trends Neurosci. 1993; 16:278–283. [PubMed: 7689772]

Kistner U, Wenzel BM, Veh RW, Cases-Langhoff C, Garner AM, Appeltauer U, Voss B, Gundelfinger ED, Garner CC. SAP90, a rat presynaptic protein related to the product of the *Drosophila* tumor suppressor gene *dlg-A*. J. Biol. Chem. 1993; 268:4580–4583. [PubMed: 7680343]

Koch CA, Anderson D, Moran MF, Ellis C, Pawson T. SH2 and SH3 domains: elements that control interactions of cytoplasmic signaling proteins. Science. 1991; 252:668–674. [PubMed: 1708916]

Laemmli UK. Cleavage of structural proteins during the assembly of the head of bacteriophage T4. Nature. 1970; 267:680–685. [PubMed: 5432063]

Littleton JT, Stern M, Schulze K, Perin M, Bellen HJ. Mutational analysis of Drosophila *synaptotagmin* demonstrates its essential role in Ca^{2+}-activated neurotransmitter release. Cell. 1993; 74:1125–1134. [PubMed: 8104705]

Mayer BJ, Hamaguchi M, Hanafusa H. A novel viral oncogene with structural similarity to phospholipase C. Nature. 1988; 332:272–275. [PubMed: 2450282]

Pawson T, Gish CD. SH2 and SH3 domains: from structure to function. Cell. 1992; 71:359–362. [PubMed: 1423600]

Perin MS, Johnston PA, Ozcelik T, Jahn R, Francke U, Südhof TC. Structural and functional conservation of synaptotagmin (p65) in *Drosophila* and humans. J. Biol. Chem. 1991; 266:615–622. [PubMed: 1840599]

Perrimon N. The maternal effect of *lethal(1) discs-large-1*: a recessive oncogene of *Drosophila melanogaster*. Dev. Biol. 1988; 127:392–407. [PubMed: 3132409]

Ramirez F, Boast S, D'Alessio M, Lee B, Prince J, Su MW, Vissing H, Yoshioka H. Fibrillar collagen genes. Structure and expression in normal and diseased states. Ann. NY Acad. Sci. 1990; 580:74–80. [PubMed: 2186697]

Ridley AJ, Hall A. The small GTP-binding protein rho regulates the assembly of focal adhesions and actin stress fibers in response to growth factor. Cell. 1992; 70:389–399. [PubMed: 1643657]

Ridley AJ, Paterson HF, Johnston CL, Diekermann D, Hall A. The small CTP-binding protein rat regulates growth factor-induced membrane ruffling. Cell. 1992; 70:401–410. [PubMed: 1643658]

Smith MR, Matthews NT, Jones KA, Kung H-F. Biological actions of oncogenes. Pharmacol. Ther. 1993; 58:211–236. [PubMed: 8415879]

Stewart M, Murphy C, Fristrom JW. The recovery and preliminary characterization of X chromosome mutants affecting imaginal discs of *Drosophila melanogaster*. Dev. Biol. 1972; 27:71–83. [PubMed: 4621757]

Südhof TC, Jahn R. Proteins of synaptic vesicles involved in exocytosis and membrane recycling. Neuron. 1991; 6:665–677. [PubMed: 1673848]

Ushkaryov YA, Petrenko AC, Geppert M, Südhof TC. Neurexins: synaptic cell surface proteins related to the α-latrotoxin receptor and laminin. Science. 1992; 257:50–56. [PubMed: 1621094]

Willott E, Balda MS, Fanning AS, Jameson B, Van Itallie C, Anderson JM. The tight junction protein ZO-1 is homologous to the *Drosophila* disc-large tumor suppressor protein of septate junctions. Proc. Natl. Acad. Sci. USA. 1993; 90:7834–7838. [PubMed: 8395056]

Woods DF, Bryant PJ. Molecular cloning of the *lethal(1) discs large-1* oncogene of *Drosophila*. Dev. Biol. 1989; 134:222–235. [PubMed: 2471660]

Woods DF, Bryant PJ. The disc-large tumor suppressor gene of Drosophila encodes aguanylate kinase homolog localized at septate junctions. Cell. 1991; 66:451–464. [PubMed: 1651169]

Woods DF, Bryant PJ. ZO-1, DlgA and PSD-95/SAP90: homologous proteins in tight, septate and synaptic cell junctions. Mech. Dev. 1993a; 44:85–89. [PubMed: 8155583]

Woods DF, Bryant PJ. Apical junctions and cell signalling in epithelia. J. Cell Sci. 1993b; 17:171–181.

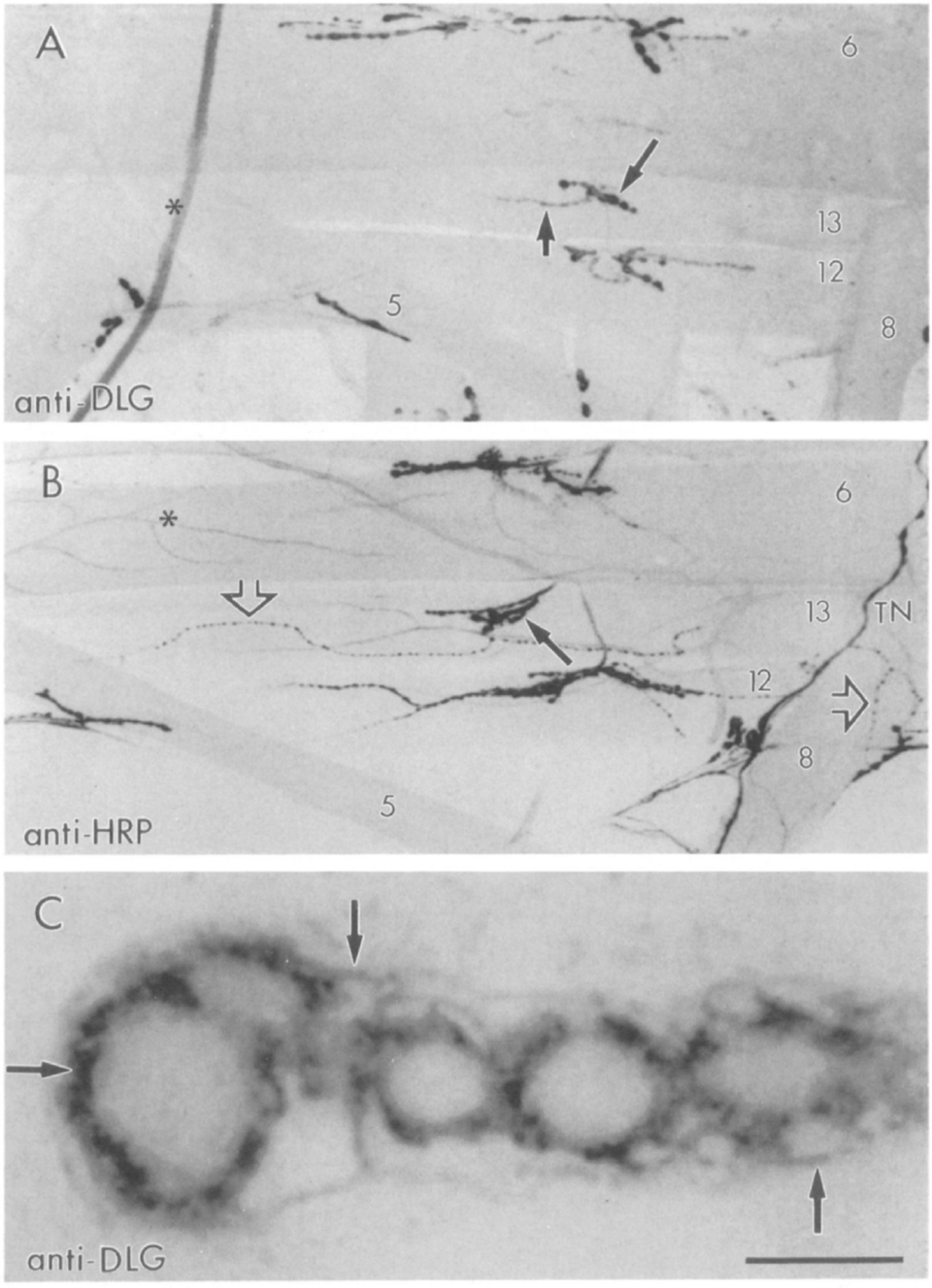

Figure 1. Confocal Micrographs of dlg- and HRP-Like Immunoreactivity at the Body Wall Muscles of Wild-Type Drosophila Larvae

(A) Type Ib synaptic boutons stain with anti-dlg antibodies (long arrow). Type Is boutons also stain (short arrow), but to a lesser degree.

(B) Neuromuscular junctions stained with anti-HRP antibodies, which stain all bouton types. Note the presence of type II boutons (open arrows) in a subset of muscles. Long arrow points to a type Ib bouton in muscle 13. Asterisk marks a branching trachiole.

(C) High magnification view of dlg-like immunoreactivity in a string of type Ib boutons at muscle 6. Focus was at the midlevel of the boutons. Arrows point to the perisynaptic network. TN, transverse nerve. Scale bar equals 90 μm in (A) and (B), 5 μm in (C).

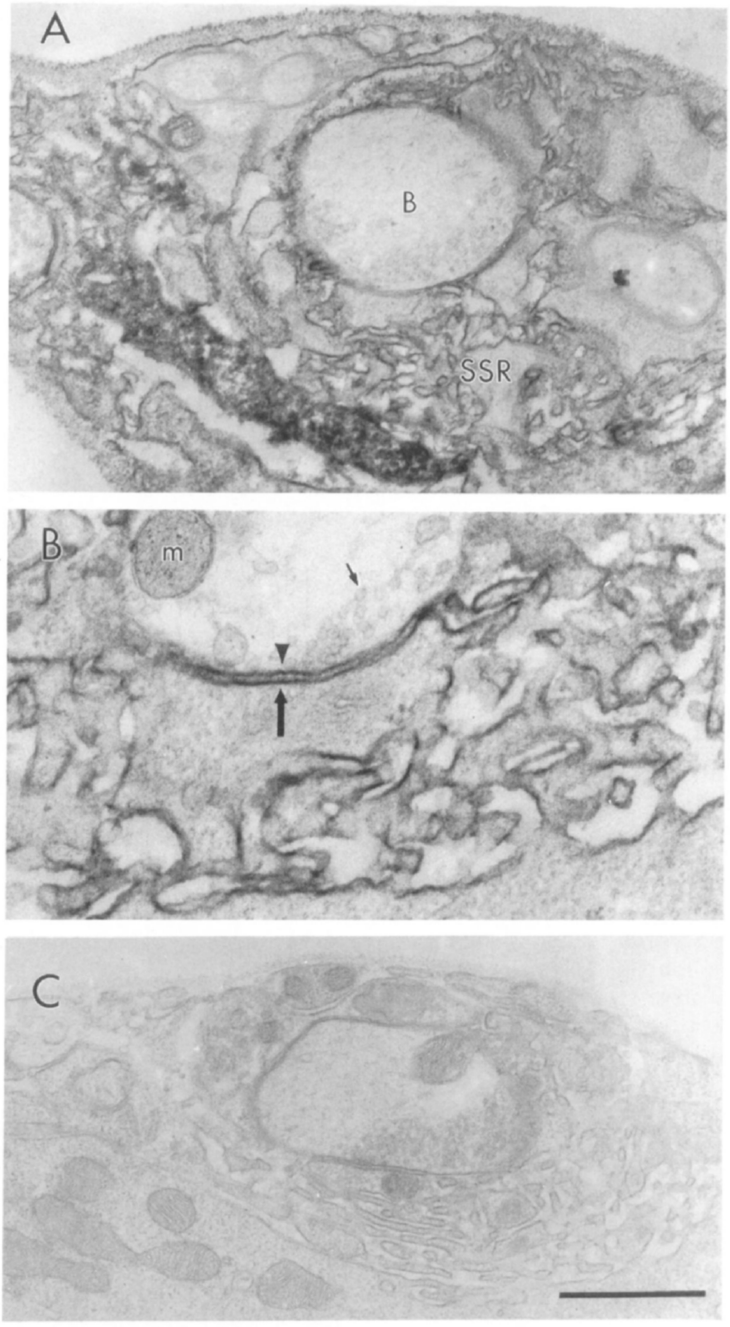

Figure 2. Immunolocalization of dlg at Type Ib Boutons

(A) Type Ib boutons (indicated with a B) at muscle 6 showing immunoreactivity associated with the SSR. (B) High magnification view of the presynaptic (arrowhead) and postsynaptic (large arrow) membrane, and the associated immunoreactivity. Note that immunoreactivity is concentrated at the SSR, and to a lesser extent, to the presynaptic bouton border. Small arrow indicates a synaptic vesicle. Immunoreactivity was visualized using the peroxidase reaction with DAB as a substrate in samples fixed with paraformaldehyde and 0.01%

glutaraldehyde. m, mitochondria. (C) Type Ib bouton from a control sample in which the primary antibody was omitted. Scale bar equals 1 μm in (A) and (C), 0.43 μm in (B).

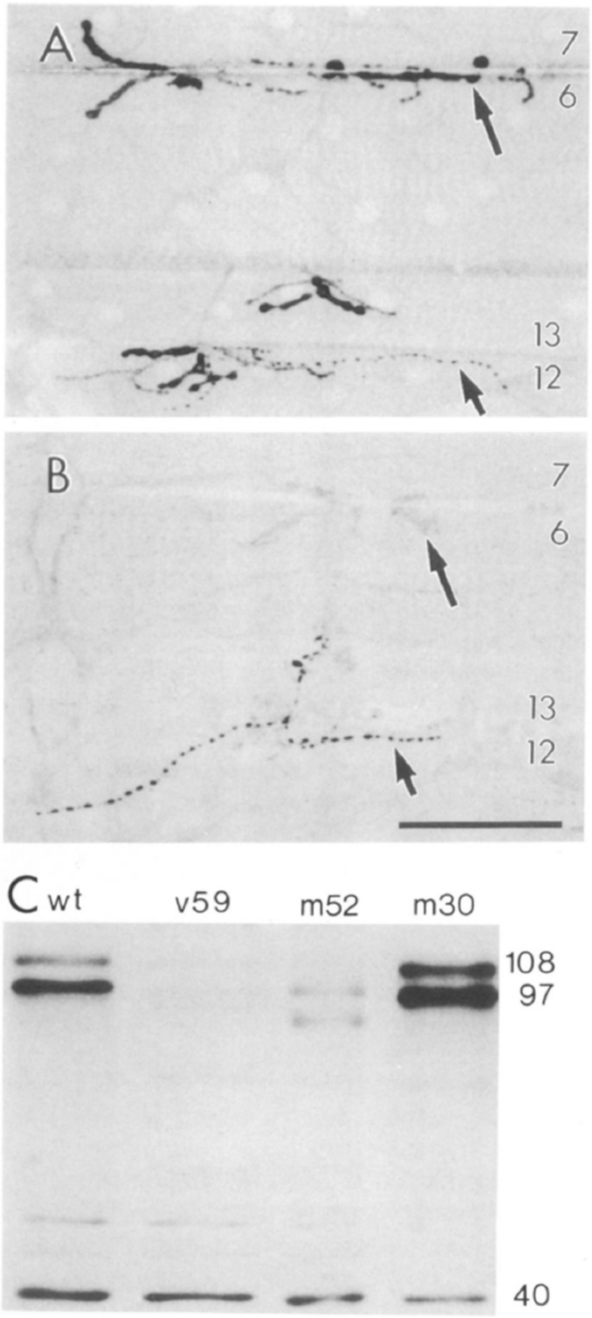

Figure 3. dlg Expression in *dlg* Mutants and Western Blot Analysis of dlg Expression at the Body Wall Muscles

(A) A wild-type sample showing dlg staining at type Ib boutons (long arrow) at muscles 6 7, 12, and 13, and type III boutons at muscle 12 (short arrow).

(B) A dlg^{m52}/Df sample showing muscles 6, 7, 12, and 13, which are almost devoid of immunoreactivity at type Ib boutons. Note that immunoreactivity at type III boutons is not affected in the mutant. Image acquisition and processing parameters were identical for wild-type and mutant samples.

(C) Western blot of body wall muscles of wild-type and *dlg* mutants. Each lane was loaded with 2 μg of protein. Lane 1, wild type; lane 2, dlg^{v59}/Df; lane 3, dlg^{m52}/Df; lane 4, dlg^{m30}/Df. Molecular masses of intensely stained bands are indicated to the right in kilodaltons. Scale bar equals 50 μ in (A) and 80 μm in (B).

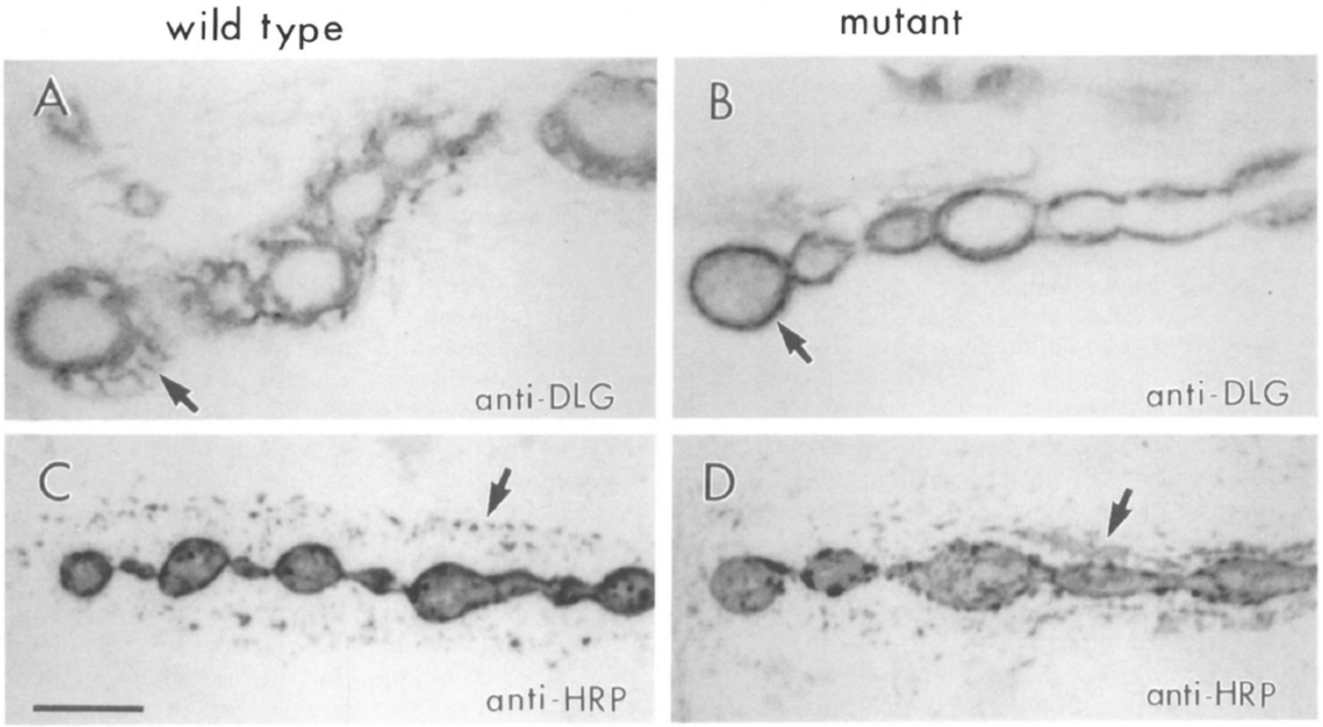

Figure 4. Staining of Type Ib Boutons Is Altered in *dlg* Mutants

(A and B) Anti-dlg staining at muscle 6 type Ib boutons in wild-type (A) and dlg^{v59}/Df mutant (B) samples. This *dlg* allele still exhibits immunoreactivity, though somewhat reduced. Note the concentration of staining at the bouton rim (arrow) and the lack of perisynaptic signal in the mutant.

(C and D) Anti-HRP staining at muscle 6 in wild-type (C) and dlg^{v59}/Df mutant (D) sample. The punctate anti-HRP staining at the perisynaptic network in wild type (arrow) evenly surrounds the string of boutons. In the mutant, immunoreactive material is irregularly distributed with large clumps (arrow) forming at various locations. Scale bar equals 5 μm.

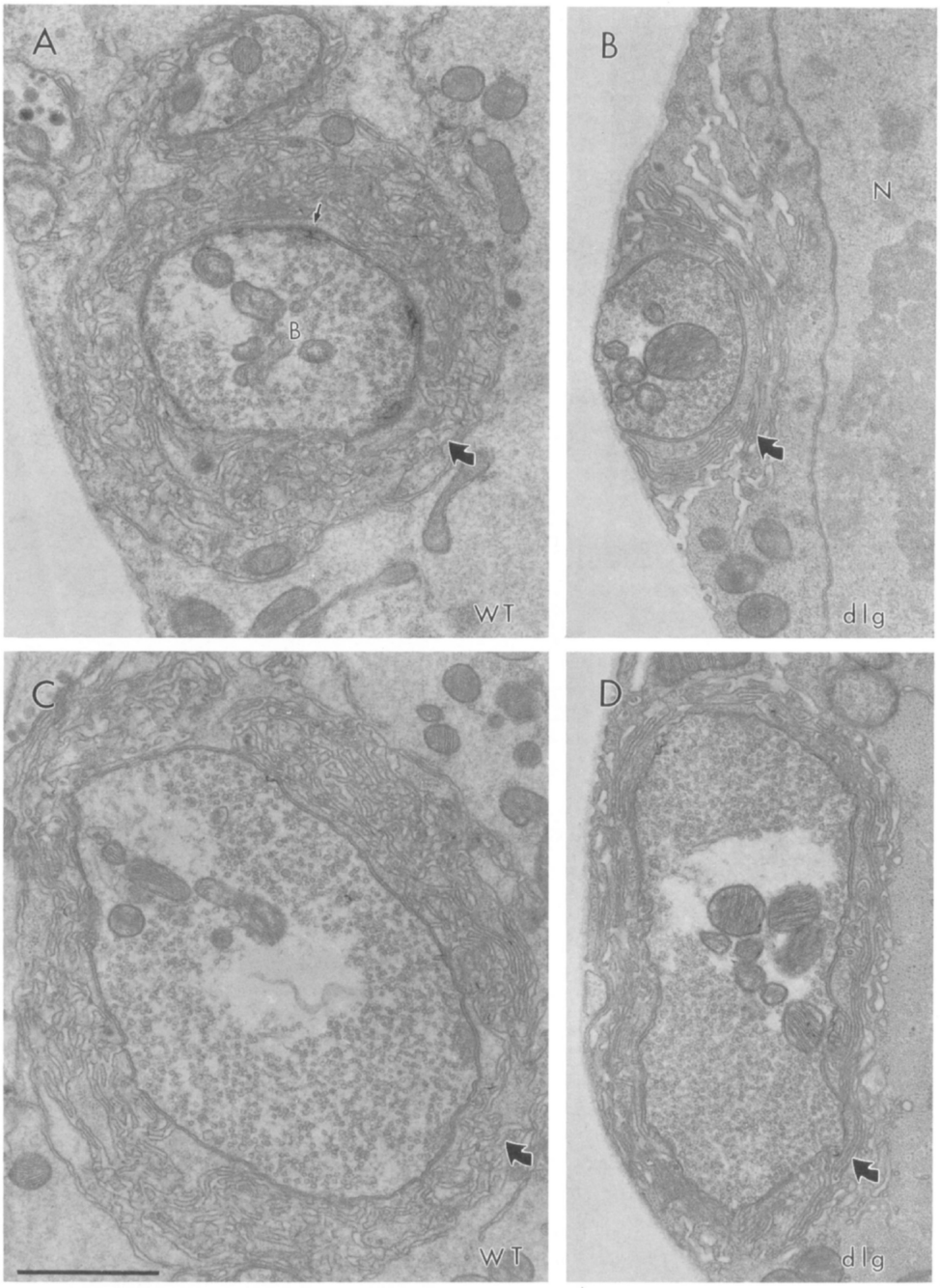

Figure 5. Synaptic Ultrastructure Is Altered in *dlg* Mutants

(A and C) Ultrastructure of type Ib synaptic boutons in wild type. Note the abundant 40 nm clear vesicles, a presynaptic density (thin arrow), and the SSR localized around the presynaptic bouton (thick arrow).

(B and D) Ultrastructure of typical type Ib boutons in dlg^{v59}/Df. Note that the SSR is less convoluted than in the wild type. N, nucleus; B, bouton. Scale bar equals 1 μm.

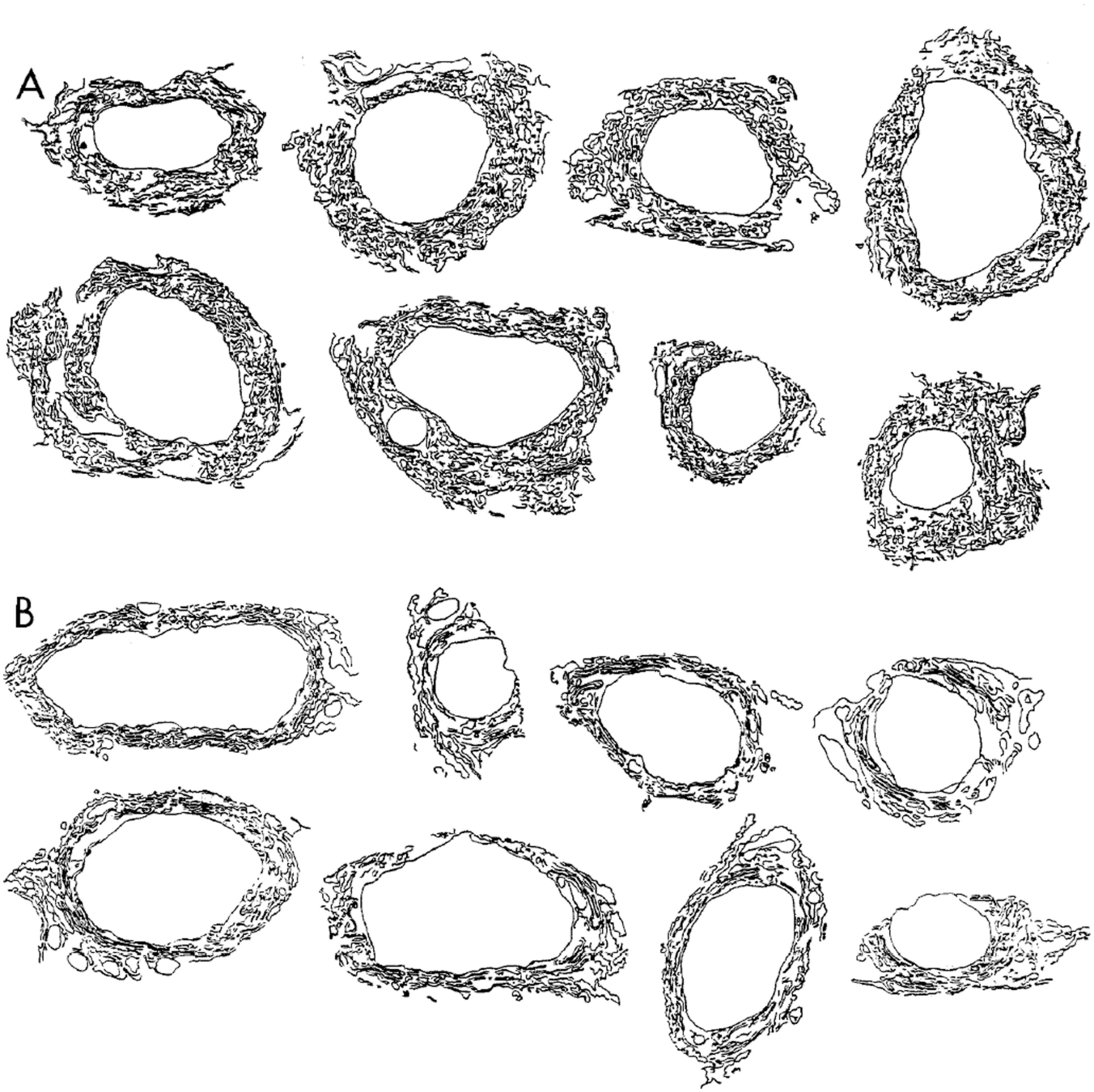

Figure 6. Alterations in the SSR in *dlg* Mutants

(A) Subsynaptic reticulum in eight different type Ib boutons from control samples.

(B) Subsynaptic reticulum in eight type Ib boutons in *dlg* mutants. These drawings were obtained by tracing the SSR membranes from micrographs of a thin transversal section through the midline of the boutons. Note that the SSR is less extensive in the mutants, and the degree of membrane convolution is reduced.

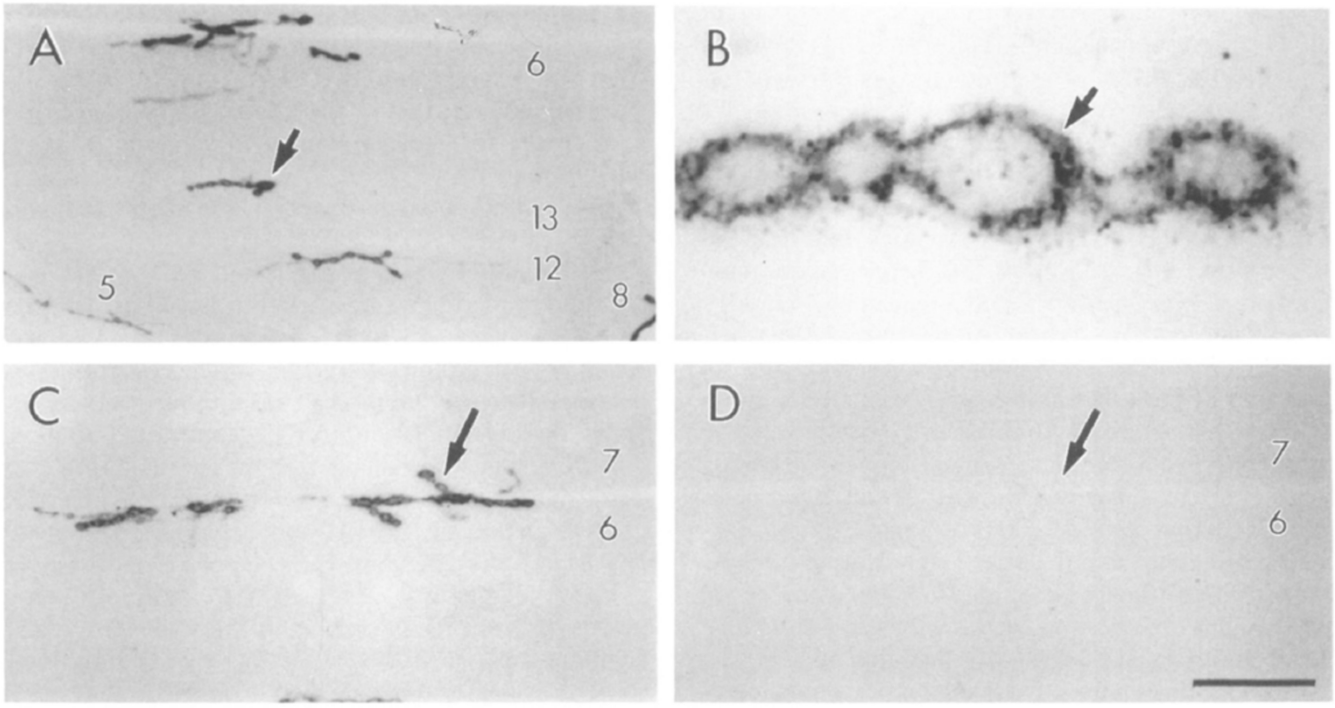

Figure 7. PSD-95-Like Immunoreactivity at Type I Boutons

(A) Immunoreactivity at wild-type neuromuscular junctions.

(B) High magnification view of type Ib boutons stained with anti-PSD-95 antibodies at muscle fiber 6.

(C and D) Elimination of immunoreactivity at type I boutons in dlg^{m52}/Df. (C) Control sample showing immunoreactivity at muscles 6 and 7. (D) Similar view of a dlg^{m52}/Df sample. Image acquisition and processing parameters were identical for wild-type and mutant samples. Scale bar equals 65 μm in (A), 5 μm in (B), and 45 μm in (C) and (D).